Organic LETTERS
Letter
pubs.acs.org/OrgLett

The Effects of Cyclic Conjugation and Bending on the Optoelectronic Properties of Paraphenylenes

Penghao Li, Thomas J. Sisto, Evan R. Darzi, and Ramesh Jasti*

Department of Chemistry and Division of Materials Science and Engineering, Boston University, Boston, Massachusetts 02215, United States

Supporting Information

ABSTRACT: Cycloparaphenylenes (CPPs) have optoelectronic properties that are unique when compared to their acyclic oligoparaphenylene counterparts. The synthesis and characterization of two bent heptaphenyl-containing macrocycles has been achieved in order to probe the effects of bending and cyclic conjugation on the properties of the CPPs. The study suggests that both bending and cyclic conjugation play a role in the novel properties of the CPPs.

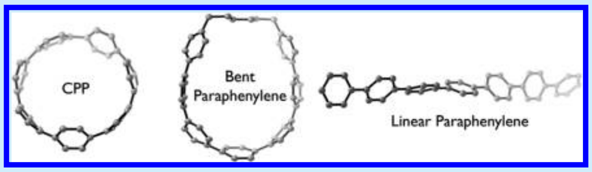

The [*n*]cycloparaphenylenes (CPPs) are structurally unique macrocycles consisting of *n* para-linked benzene units (Figure 1). Since first synthesized and characterized in 2008, numerous routes to a variety of [*n*]CPPs have been reported by the Jasti,[1] Itami,[2] and Yamago[3] laboratories. Although often cited for their potential application in the bottom-up growth of uniform carbon nanotubes,[4] the CPPs have unique optoelectronic properties in their own right. As new conjugated organic materials, the CPPs are attractive due to their size-dependent optoelectronic properties,[1a,b,3b] as well as their guest–host properties[1d,5] and highly porous solid state structures.[1e,2b,c,3c] The CPPs have increasing HOMO energies and decreasing LUMO energies (narrowing band gap) with decreasing molecular size.[3b] This behavior is exactly opposite to that observed in the case of acyclic paraphenylenes.[6] In addition, the solubility of the CPPs is vastly improved as compared to the linear oligoparaphenylenes, presumably due to differences in the number of intermolecular $\pi-\pi$ contacts accessible when comparing nonplanar compounds to flat linear compounds (*vide infra*). All known CPPs (sizes [6]–[18]CPP) are soluble, while unsubstituted paraphenylenes larger than sexiphenyl are completely insoluble.[7]

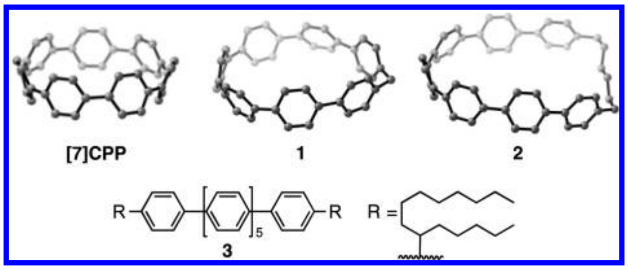

Figure 1. DFT optimized geometries of [7]CPP, **1**, and **2**, along with previously reported linear heptaphenyl **3**.[6b]

When rationalizing the origin of the unique optoelectronic properties of the CPPs versus acyclic oligoparaphenylenes, the most obvious structural differences are the bent phenylene units, the cyclic conjugation, and the smaller torsional angles of the CPPs.[8] A fundamental understanding of the effects that structure has on optoelectronic properties is paramount when designing better-performing conjugated organic materials.[8,9] To probe the effects these structural characteristics have on the properties of the CPPs, we have synthesized alkyl-tethered heptaphenyl-containing macrocycles **1** and **2** (Figure 1). Drawing inspiration from the related studies by Bodwell and co-workers,[10] we recognized that we can systematically vary the degree of bending of the heptaphenyl moiety through the insertion of various length alkyl chains into the backbone of a macrocycle. This alkyl tether also serves to break the conjugation of the macrocycle. Comparison of [7]CPP to macrocycle **1** by cyclic voltammetry, absorption, and fluorescence experiments allows for an approximation of the effect of cyclic conjugation due to their similar degrees of bending and torsional angles (*vide infra*). Comparison of **1**, **2**, and linear heptaphenyl **3** allows for insight into the effects of bending. Herein, we report the syntheses and characterization of **1** and **2** in order to gain insight into these phenomena.

Our strategy for the synthesis of **1** and **2** relies upon the 3,6-*syn*-dimethoxycyclohexa-1,4-diene moieties of fragment **6** as masked arene units to provide the curvature necessary for a macrocyclization reaction with tethers **9** and **10** (Schemes 1 and 2). Subsequent aromatization of the resultant macrocycles would lead to **1** and **2**. To synthesize **6**, we began with a lithium halogen exchange of **4**[1b] followed by addition of monoketal protected benzoquinone (Scheme 1). Subsequent deprotection of the crude reaction mixture at room temperature with 10% aqueous acetic acid yields hydroxy ketone **5** in 90% yield over two steps. Deprotonation of **5** with NaH at −78 °C leads to a charged sodium alkoxide that directs the addition of lithiated 1,4-bromochlorobenzene in a diastereoselective manner.[1b] This

Received: November 2, 2013
Published: December 6, 2013

dx.doi.org/10.1021/ol403168x | *Org. Lett.* 2014, 16, 182−185

Scheme 1. Synthetic Route to Coupling Partners 6 and 8

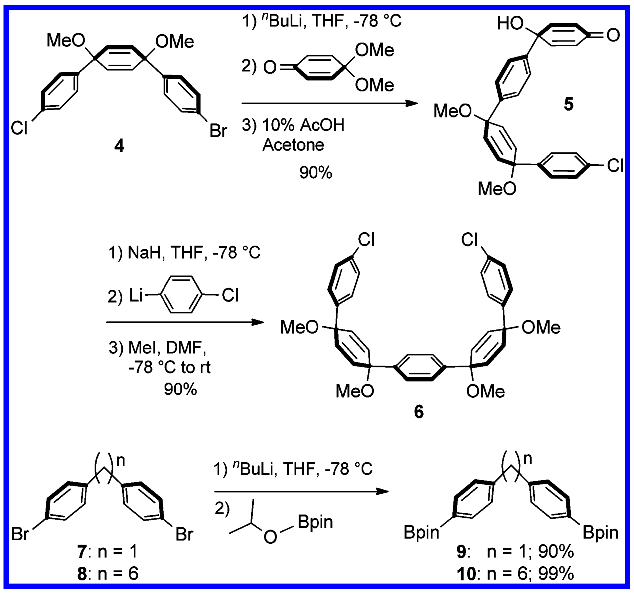

Scheme 2. Macrocyclization and Aromatization Reactions to Prepare Bent Heptaphenyls 1 and 2

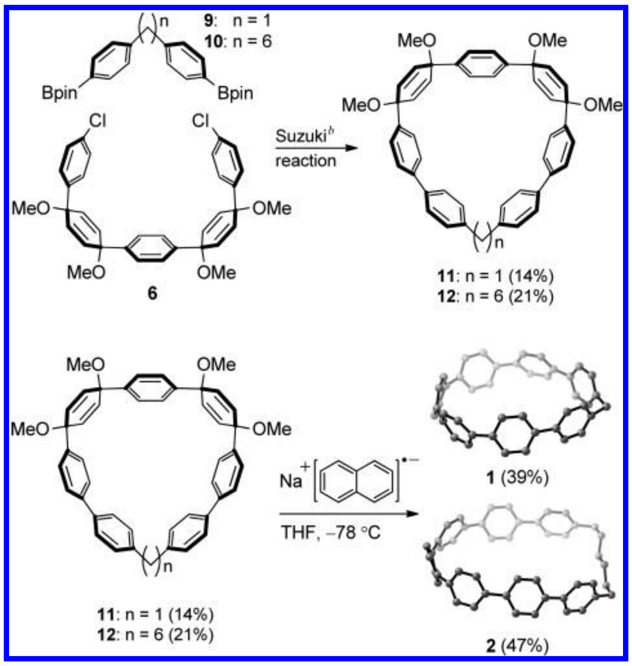

[a]Compounds 1 and 2 are represented by DFT optimized geometries. [b] Conditions: Pd(OAc)$_2$ (16 mol %), S-Phos (40 mol %), K$_3$PO$_4$ (2 equiv.), DMF/H$_2$O, 100 °C.

addition is followed by a simple iodomethane quench to lead directly to dichloride **6** in 90% yield. Notably, this synthesis can readily produce tens of grams of **6** from commercially available quionone monoketal using standard 2-L glassware. Synthesis of alkyl tethered coupling partners **9** and **10** began with dibromides **7**[11] and **8**[12] and is achieved in 90% and 99% yield, respectively, through simple lithium halogen exchange and subsequent quench with isopropoxyboronic acid pinacol ester (Scheme 1).

With the necessary fragments in hand, we turned our attention to preparing the macrocyclic precursors to structures **1** and **2**. A Suzuki coupling[13] of dichloride **6** and either bisboronate **9** or **10** formed macrocycles **11** and **12** in 14% and 21% yield, respectively. The yields are predictably low due to the high strain of the macrocycles and the indiscriminate nature of the coupling reaction, which leads to high amounts of oligomerization. Subjecting macrocycles **11** and **12** to single electron reductant sodium napthalenide at −78 °C gives bent heptaphenyls **1** and **2** in 39% and 47% yield, respectively. Characterization by NMR (^{1}H and ^{13}C), IR, and MALDI-TOF confirmed the structural assignment.[14]

With the syntheses complete, we next probed the electronic differences between each molecule utilizing cyclic voltammetry (Table 1).[14] Similar to all CPPs, [7]CPP shows a reversible peak in the negative potential range corresponding to a reduction wave with a half-wave potential of −2.57 V (vs Fc/Fc^{+}), along with a reversible peak in the possitive potential range, corresponding to an oxidation wave with a half-wave potential of 0.53 V (vs Fc/Fc^{+}). Compound **1** exhibits a quasi-reversible peak corresponding to a reduction wave; however, the half-wave potential is significantly higher at −2.74 V (vs Fc/Fc^{+}). Additionally, the oxidation of **1** is irreversible with an onset potential at 0.63 V (vs Fc/Fc^{+}). Since macrocycle **1** contains phenylene units that are bent to a similar extent as [7]CPP and the torsional angles between phenyl units are also similar (*vide infra*), one can conclude that cyclic conjugation plays a substantial role in raising the HOMO and lowering the LUMO in the CPPs. Similar to macrocycle **1**, structure **2** has a quasi-reversible peak corresponding to a reduction wave with a half-wave potential at −2.75 V (vs Fc/Fc^{+}) and an irreversible peak corresponding to an oxidation wave with an onset potential of 0.71 V (vs Fc/Fc^{+}). Macrocycles **1** and **2** are very similar with only a slight increase in potentials as compared to the difference between [7]CPP and **1**. The oxidation potential of **3**, as reported by Rathore,[6a] shows a first half-wave of 1.4 V versus SCE, which correlates to a half-wave potential of 1 V versus Fc/Fc^{+}. This large difference in oxidation potentials between **2** and **3** provides experimental evidence for bending in oligophenylenes also leading to a narrowing of band gaps (i.e., raising of the HOMO and lowering of the LUMO).

Table 1. Cyclic Voltammetry Data[a] for [7]CPP, 1, 2, and 3

entry	E_{red} (V) (half-wave)	E_{ox} (V) (onset)
[7]CPP	−2.57	0.47
1	−2.74	0.63
2	−2.75	0.71
3[6b]	N/A	1.0

[a]V versus ferrocene/ferrocenium couple.

Next we investigated the UV−vis and fluorescence spectra of the new bent heptaphenyl-containing macrocycles for comparison with [7]CPP. Macrocycle **1** displayed an absorption maximum of 321 nm along with a small shoulder peak at 390 nm (Figure 2 and Table S1). The extinction coeffecients for these features are 5.15×10^4 and 0.814×10^4 M^{-1} cm^{-1}, respectively. Macrocycle **2** has a similar absorption pattern, displaying one large absorption maximum and one smaller shoulder peak ($\lambda_{abs1} = 319$ nm, $\varepsilon_1 = 4.45 \times 10^4$ M^{-1} cm^{-1}; $\lambda_{abs2} = 375$ nm, $\varepsilon_2 = 1.43 \times 10^4$ M^{-1} cm^{-1}). For comparison, [7]CPP displays an absorption maximum at 340 nm ($\varepsilon = 6.58 \times 10^4$ M^{-1} cm^{-1}) along with a very weak shoulder peak at 408 nm ($\varepsilon = 0.316 \times 10^4$ M^{-1} cm^{-1}). Linear heptaphenyl **3** displays a single absorption at 326 nm with an extinction coefficient of 9.16×10^4 M^{-1} cm^{-1}.[6b] Notably, the HOMO−LUMO

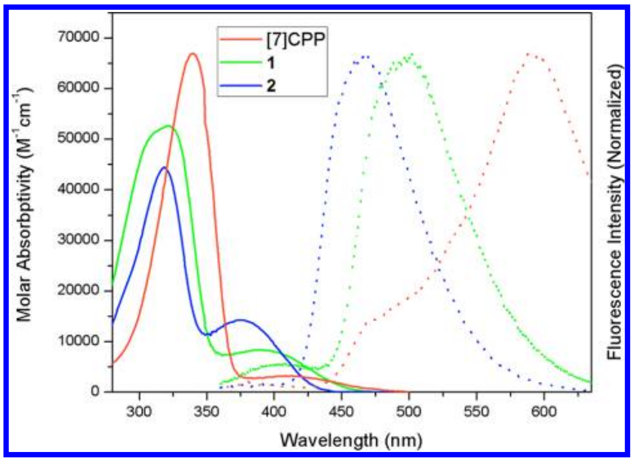

Figure 2. UV−vis absorption and fluorescence data for [7]CPP, **1**, and **2**.

transition that is forbidden in the CPPs (the minor red-shifted absorption) becomes more prominent as symmetry is broken by the alkyl tether.[8,15] A large difference also exists between the wavelengths of the HOMO−LUMO transitions of the bent molecules when compared to the linear paraphenylene, consistent with cyclic voltammetry data. TD-DFT calculations confirm this trend by showing that the $\lambda_{\text{HOMO-LUMO}}$ blue shifts while the oscillator strength increases moving from [7]CPP through the methylene spaced heptaphenyl macrocycles (1−20 methylenes).[16] Fluorescence data were also collected for each of the final compounds (Figure 2 and Table S1). [7]CPP displays a weak fluorescence emission at 588 nm ($\phi_f = 0.006$), while **1** and **2** emit strongly at blue-shifted values of 502 nm ($\phi_f = 0.23$) and 469 nm ($\phi_f = 0.25$). Acyclic analogue **3** is reported to emit at 408 nm, interestingly with a much higher quantum yield of 1.0.[6b]

In order to further understand the molecular geometry and electronic structures of this class of molecules, we performed theoretical calculations for bent heptaphenyls with methylene tether lengths from 1 to 20 carbons (Figure 3).[17] [7]CPP and linear *p*-heptaphenyl were also calculated for comparison. Predictably, as the tether is increased in size the heptaphenyl becomes less bent. As this occurs, the HOMO energies decrease while the LUMO energies increase, though structural anomalies provide small fluctuations within the larger overall trend. In addition, we observe a trend of slightly increasing average torsional angles when moving from [7]CPP to macrocycle **1** to macrocycle **2** to acyclic analogue heptaphenyl (25.5°, 29.9°, 30.3°, and 36.3°, respectively). When the data was evaluated, the most important finding was the significant difference between the band gap of [7]CPP and that of any tethered macrocycle, presumably due to cyclic conjugation. Furthermore, another large difference exists between the HOMO energy levels of the largest tethered macrocycle and linear heptaphenyl.

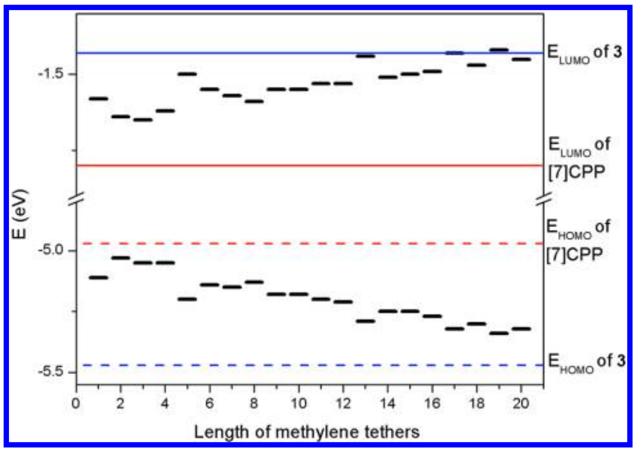

Figure 3. DFT calculated HOMO and LUMO energies for [7]CPP, linear heptaphenyl, heptaphenyl macrocycles with tether lengths from 1 to 20 methylenes.

In the past five years, the cycloparaphenylenes have become synthetically accessible in various sizes and on gram scale. Throughout the development of these syntheses, characterization of the optoelectronic properties of the cycloparaphenylenes has revealed striking differences when compared to acyclic paraphenylenes. We have demonstrated experimentally that there are two structural features, bending and cyclic conjugation, that play a prominent role in the optoelectronic differences between the CPPs and OPPs. By breaking the cyclic conjugation of [7]CPP with one methylene, we have shown that this similarly bent heptaphenyl **1** is significantly harder to oxidize and reduce. Decreasing the bending of the heptaphenyl unit by increasing the macrocycle tether length results in a minor increase in the oxidation and reduction potentials. Similarly, we have shown that bent heptaphenyl has substantially different optical properties compared to acyclic heptaphenyl, while being much easier to oxidize and reduce. This series of compounds has allowed for the experimental demonstration that the bending and cyclic conjugation of the CPPs provide optoelectronic characteristics and solubility rendering them novel building blocks to new conjugated organic materials.

■ ASSOCIATED CONTENT

Ⓢ Supporting Information

Detailed experimental procedures and characterizations for all the compounds, cyclic voltammetry spectra, optical data, and calculation details. This material is available free of charge via the Internet at http://pubs.acs.org.

■ AUTHOR INFORMATION

Corresponding Author

*E-mail: jasti@bu.edu.

Notes

The authors declare no competing financial interest.

■ ACKNOWLEDGMENTS

We thank the Alfred P. Sloan Foundation for financial support.

■ REFERENCES

(1) (a) Jasti, R.; Bhattacharjee, J.; Neaton, J. B.; Bertozzi, C. R. *J. Am. Chem. Soc.* **2008**, *130*, 17646−17647. (b) Sisto, T. J.; Golder, M. R.; Hirst, E. S.; Jasti, R. *J. Am. Chem. Soc.* **2011**, *133*, 15800−15802. (c) Darzi, E. R.; Sisto, T. J.; Jasti, R. *J. Org. Chem.* **2012**, *77*, 6624−6628. (d) Xia, J.; Bacon, J. W.; Jasti, R. *Chem. Sci.* **2012**, *3*, 3018−3021. (e) Xia, J.; Jasti, R. *Angew. Chem., Int. Ed.* **2012**, *51*, 2474−2476. (f) Hirst, E. S.; Jasti, R. *J. Org. Chem.* **2012**, *77*, 10473−10478.

(2) (a) Takaba, H.; Omachi, H.; Yamamoto, Y.; Bouffard, J.; Itami, K. *Angew. Chem., Int. Ed.* **2009**, *48*, 6112−6116. (b) Segawa, Y.; Miyamoto, S.; Omachi, H.; Matsuura, S.; Senel, P.; Sasamori, T.; Tokitoh, N.; Itami, K. *Angew. Chem., Int. Ed.* **2011**, *50*, 3244−3248.

(c) Segawa, Y.; Senel, P.; Matsuura, S.; Omachi, H.; Itami, K. *Chem. Lett.* **2011**, *40*, 423−425. (d) Ishii, Y.; Nakanishi, Y.; Omachi, H.; Matsuura, S.; Matsui, K.; Shinohara, H.; Segawa, Y.; Itami, K. *Chem. Sci.* **2012**, *3*, 2340−2345.

(3) (a) Yamago, S.; Watanabe, Y.; Iwamoto, T. *Angew. Chem., Int. Ed.* **2010**, *49*, 757−759. (b) Iwamoto, T.; Watanabe, Y.; Sakamoto, Y.-I.; Suzuki, T.; Yamago, S. *J. Am. Chem. Soc.* **2011**, *133*, 8354−8361. (c) Kayahara, E.; Sakamoto, Y.; Suzuki, T.; Yamago, S. *Org. Lett.* **2012**, *14*, 3284−3287. (d) Kayahara, E.; Iwamoto, T.; Suzuki, T.; Yamago, S. *Chem. Lett.* **2013**, *42*, 621−623.

(4) (a) Bunz, U. H. F.; Menning, S.; Martín, N. *Angew. Chem., Int. Ed.* **2012**, *51*, 7094−7101. (b) Fort, E. H.; Scott, L. T. *J. Mater. Chem.* **2011**, *21*, 1373−1381. (c) Schrettl, S.; Frauenrath, H. *Angew. Chem., Int. Ed.* **2012**, *51*, 6569−6571. (d) Jasti, R.; Bertozzi, C. R. *Chem. Phys. Lett.* **2010**, *494*, 1−7.

(5) (a) Iwamoto, T.; Watanabe, Y.; Sadahiro, T.; Haino, T.; Yamago, S. *Angew. Chem., Int. Ed.* **2011**, *50*, 8342−8344 (S8342/1−S8342/20). (b) Iwamoto, T.; Watanabe, Y.; Takaya, H.; Haino, T.; Yasuda, N.; Yamago, S. *Chem.—Eur. J.* **2013**, *19*, 14061−14068.

(6) (a) Nijegorodov, N. I.; Downey, W. S.; Danailov, M. B. *Spectrochim. Acta, Part A* **2000**, *56*, 783−795. (b) Banerjee, M.; Shukla, R.; Rathore, R. *J. Am. Chem. Soc.* **2009**, *131*, 1780−1786.

(7) Meerholz, K.; Heinze, J. *Electrochim. Acta* **1996**, *41*, 1839−1854.

(8) Segawa, Y.; Fukazawa, A.; Matsuura, S.; Omachi, H.; Yamaguchi, S.; Irle, S.; Itami, K. *Org. Biomol. Chem.* **2012**, *10*, 5979−5984.

(9) (a) Fujitsuka, M.; Cho, D. W.; Iwamoto, T.; Yamago, S.; Majima, T. *Phys. Chem. Chem. Phys.* **2012**, *14*, 14585−14588. (b) Fujitsuka, M.; Iwamoto, T.; Kayahara, E.; Yamago, S.; Majima, T. *ChemPhysChem* **2013**, *14*, 1570−1572. (c) Chen, H.; Golder, M. R.; Wang, F.; Jasti, R.; Swan, A. K. *Carbon* **2013**, DOI: 10.1016/j.carbon.2013.09.082. (d) Nishihara, T.; Segawa, Y.; Itami, K.; Kanemitsu, Y. *J. Phys. Chem. Lett.* **2012**, *3*, 3125−3128.

(10) Some selected publications from the Bodwell group: (a) Bodwell, G. J.; Bridson, J. N.; Chen, S.-L.; Poirier, R. A. *J. Am. Chem. Soc.* **2001**, *123*, 4704−4708. (b) Bodwell, G. J.; Miller, D. O.; Vermeij, R. J. *Org. Lett.* **2001**, *3*, 2093−2096. (c) Bodwell, G. J.; Bridson, J. N.; Cyrañski, M. K.; Kennedy, J. W. J.; Krygowski, T. M.; Mannion, M. R.; Miller, D. O. *J. Org. Chem.* **2003**, *68*, 2089−2098. (g) Merner, B. L.; Dawe, L. N.; Bodwell, G. J. *Angew. Chem., Int. Ed.* **2009**, *48*, 5487−5491. (h) Merner, B. L.; Unikela, K. S.; Dawe, L. N.; Thompson, D. W.; Bodwell, G. J. *Chem. Commun.* **2013**, *49*, 5930−5932.

(11) Tour, J. M.; Rawlett, A. M.; Kozaki, M.; Yao, Y.; Jagessar, R. C.; Dirk, S. M.; Price, D. W.; Reed, M. A.; Zhou, C.-W.; Chen, J.; Wang, W.; Campbell, I. *Chem.—Eur. J.* **2001**, *7*, 5118−5134.

(12) Cammidge, A. N.; King, A. S. H. *Tetrahedron Lett.* **2006**, *47*, 5569−5572.

(13) Barder, T. E.; Walker, S. D.; Martinelli, J. R.; Buchwald, S. L. *J. Am. Chem. Soc.* **2005**, *127*, 4685−4696.

(14) See Supporting Information for details.

(15) For detailed theoretical analysis, see: (a) Wong, B. M. *J. Phys. Chem. C* **2009**, *113*, 21921−21927. (b) Camacho, C.; Niehaus, T. A.; Itami, K.; Irle, S. *Chem. Sci.* **2013**, *4*, 187−195.

(16) See Supporting Information for details.

(17) Calculations were performed by using density function theory (DFT) at the B3LYP/6-31* level of theory.